Understanding Metal Synergy in Heterodinuclear Catalysts for the Copolymerization of CO_2 and Epoxides

*Arron C. Deacy,[a] Alexander F. R. Kilpatrick,[a] Anna Regoutz[b] and Charlotte K. Williams[a]**

[a]Department of Chemistry, University of Oxford, Chemistry Research Laboratory, 12 Mansfield Road, Oxford, OX1 3TA, U.K.

[b]Department of Materials, Imperial College London, London, SW7 2AZ, U.K.

*Corresponding author: charlotte.williams@chem.ox.ac.uk

Abstract

The copolymerization of carbon dioxide with epoxides is an industrially relevant means to valorize wastes and improve sustainability in polymer manufacturing, and may also provide an economic benefit to CO2 capture and storage technologies. The efficiency of the process depends upon the catalyst used; previously Zn(II)Mg(II) heterodinuclear catalysts showed good performances at low CO_2 pressures, which has been attributed to synergic interactions between the metals. Here we report a Mg(II)Co(II) catalyst for the production of polyols by copolymerization of CO_2 with cyclohexene oxide that exhibits significantly better activity (turn-over-frequency over 12,000 h^{-1}), high CO_2 utilization (over 99 %) and high polymer selectivity (over 99 %). Detailed kinetic investigations show a second-order rate law, independent of CO_2 pressure from 1 to 40 bar. Investigations of the synergy between the metal centres showed that epoxide coordination occurs at Mg(II) with reduced transition state entropy, which the carbonate attack step is accelerated at Co(II) through lowering of the transition state enthalpy.

Society needs more and better methods to transform CO_2 into products, both to obviate industrial greenhouse gas emissions and to lock-away this recalcitrant molecule into useful products.[1] CO_2 utilization can be an important means to increase product sustainability and better understanding of its chemistry is needed to accelerate technological developments.[2-4] One promising option is its copolymerization with epoxides to yield polycarbonates (for catalysts resulting in perfectly alternating enchainment) or polyether carbonates (for catalysts resulting in less CO_2 uptake) (Fig. 1).[5-8] Life cycle analysis demonstrates a triple win in terms of greenhouse gas emissions: for every molecule of CO_2 used, two more are saved through replacing the use of the petrochemical (epoxide).[9] Some polymerization catalysts have also shown good compatibility for integration with large-scale CO_2 capture technologies and high tolerance towards common impurities found in gas streams.[10] Given the value of the polymeric products, CO_2 copolymerization could provide an economic stimulus for large-scale capture and storage technologies. This work focuses on the production of CO_2-derived polyols which are a class of polymers showing low molar mass (M_n < 5000 g mol^{-1}) but which must be hydroxyl terminated. They show equivalent or better properties than conventional polyether/ester polyols in the manufacturing of rigid and flexible foams, adhesives, elastomers and coatings.[11-14] Higher molar mass polycarbonates show properties suitable to replace petrochemicals in sectors including packaging, coatings, rigid plastics and medical materials.[11,15-17] For any application sector, the selection of the polymerization catalyst is central to process productivity and selectivity. This work describes the development and understanding of a new type of highly active heterodinuclear catalyst which exploits metal synergy.

Metal synergy is often summoned as the rationale for the high performances and activities of bimetallic catalysts but detailed mechanistic insight and support for the putative cooperative interactions are far less frequently presented.[18,19] For example, synergic interactions are invoked in mechanisms underpinning large-scale processes such as polymerization, ammonia synthesis, methanol synthesis and Fischer-Tropsch reactions as well as for organic transformations from C-H activations to redox processes but so far detailed understanding of how to design catalysts to exploit or optimize synergy is lacking.[20-23] In the field of CO_2/epoxide copolymerization, we have previously reported a series of dinuclear Zn(II)/Mg(II) catalysts and proposed their superior performances arose from synergic interactions (Fig. 1).[24] The nature of the metal combination is clearly important as a series of Zn(II)/M(I/II/III) complexes, where M= Li, Na, K, Ca, Al, Ga and In all showed inferior activity compared to the Zn(II)/Mg(II) catalyst.[25,26] This finding highlights the need for more detailed understanding and suggests there may be a special role for Mg(II) in this catalysis: it motivated the investigation of other heterodinuclear Mg(II)/M(II) complexes. We reasoned that replacing Zn(II) with Co(II), in combination with Mg(II), might increase carbonate nucleophilicity compared to Zn(II)/Mg(II) analogues and hence accelerate rates. There is less precendent for Co(II) complexes in copolymerization catalysis, although we previously observed that a di-Co(II) catalyst outperforms the di-zinc analogue.[27,28] In the mechanically related field of cyclic carbonate formation from epoxide/CO_2 coupling, Co(II) complexes are also effective.[29-31] It's important to distinguish the hypothesis that Mg/Co(II) might function synergically from the well-known Co(III) salen catalysts, which show high activity but require co-catalysts and operate by more complex multi-component mechanisms.[32-35]

Results and Discussion

Catalyst Synthesis

Previous research into heterodinuclear catalysts revealed that the mixed metal complexes are generally thermodynamically more stable than the homodinuclear counterparts.[25] Capitalizing on this finding, in this work the **MgCo** heterodinuclear complex was prepared by heating the ligand sequentially with the two metal precursors (Fig. 2a). The **MgCo** complex was isolated as a pink powder in 78 % yield and was characterized by elemental analysis and by MALDI-ToF mass spectrometry which revealed a molecular cation peak [690 Da = $[LMgCo(OAc)]^+$](Supplementary Fig. 1). The infra-red (IR) spectrum showed a series of frequencies, consistent with the molecular structure (Supplementary Fig. 2).

To allow for proper comparison in catalysis, the homodinuclear analogues, **MgMg** and **CoCo**, were prepared according to published procedures (see Supplementary Information).[27,36] A range of characterization techniques were used to assess the compounds and to establish the formation of the **MgCo** catalyst. X-ray photoelectron spectroscopy (XPS) was used to evaluate both the Co oxidation state and to confirm the sample composition (Supplementary Fig. 3). For both **CoCo** and **MgCo**, Co $2p_{1/2}$ and Co $2p_{3/2}$ core levels are observed at binding energies (BE) of 780.2 eV and 796.2 eV, respectively. In addition, satellite features at 3-5 eV higher BE are indicative of Co(II) as the oxidation state (Fig. 2b). For **MgCo** it was feasible to compare the Mg 1s and Co $2p_{3/2}$ core levels and to estimate a Mg:Co ratio of 1:1. Using SQUID measurements, the effective magnetic moments (μ_{eff}) per Co(II) centre for **MgCo** and **CoCo** were 4.75 and 4.63 μ_B, respectively (Supplementary Fig. 4). Both values are slightly higher than the spin-only value (μ_{SO} = 3.87 μ_B for S = 3/2) consistent with expected orbital contributions. Magnetic

saturation (M_{sat}) was observed at 1.94 and 2.15 μ_B for **MgCo** and **CoCo** (per Co(II) centre), at 2K respectively (Supplementary Fig. 4). These values are consistent with reported octahedral Co(II) centres showing a populated ground-state Kramers doublet.[37,38] Electrochemical measurements for **MgCo**, **CoCo** and **MgMg** were conducted using cyclic voltammetry (Supplementary Fig. 5). **MgMg** shows a series of ligand centred oxidations at potentials greater than 0.32 V (Supplementary Fig. 5). These processes are assigned to ligand-based oxidations of the phenolate rings and are analogous to previous reports of related ligands.[39-41] For **CoCo,** two separate oxidations were observed at E_{pa} = -0.34 V (Co(II/III)) and $E_{1/2}$ = -0.10 V (Co(II/III)) (Supplementary Fig. 5). The **MgCo** complex shows just one irreversible Co(II/III) oxidation at E_{pa} = -0.06 V (Fig 2c). The clear differences between the cyclic voltammograms support the formation of **MgCo**.

MgCo, **CoCo** and **MgMg** were each tested in the ROCOP of CO_2/cyclohexene oxide (CHO) at 1 bar CO_2 pressure (Table 1). The conditions for catalyst testing were optimized and for fast and selective catalysts such as **MgCo**, it is important to establish that rates are independent of stirring speed and that reactions are not under diffusion control (Supplementary Table 2). A series of experiments were conducted in the absence of and with progressively greater quantities of 1,2-cyclohexane diol (CHD) as chain transfer agent. These experiments confirm the feasibility of forming high molecular mass poly(cyclohexene carbonate) (PCHC), with the expected bimodal molecular mass distributions (Supplementary Table 2). On the other hand, the catalyst shows outstanding tolerance to protic compounds and functions highly effectively using 20 equivalents of 1,2-cyclohexane diol (CHD). Under these conditions it forms exclusively α, ω-hydroxyl telechelic PCHC, i.e. the desired polyol, and does so with a very high TOF 340 h^{-1} (0.1 mol% **MgCo**, 80 °C, 1 bar pressure CO_2). To establish the catalyst remained

thermally stable under catalytic conditions, **MgCo** was heated for 24 hours at 120 °C, in dioxane, after which both its ^{1}H NMR spectrum and performance remained identical (Supplementary Fig. 6).

Carbon Dioxide and Epoxide Copolymerization

The catalyst shows high activity and selectivity at loadings as low as 1:4000 or 0.025 mol% (catalyst:epoxide). It also shows excellent CO_2 selectivity (> 99 %) across the range of temperatures tested (80–120 °C), with no ether linkages observed by ^{1}H NMR spectroscopy. Furthermore, all polymerizations resulted only in polymer formation (i.e no cyclic carbonate) and well controlled, monomodal, polymer molar mass distributions. The catalyst functions effectively in the presence of excess chain transfer agent (1:20 catalyst:diol) resulting in the formation of polycarbonate polyols (dihydroxyl telechelic polymers). Generally the theoretically predicted molecular mass values and those obtained by GPC analysis showed good agreement (e.g. Table entry 1, M_n *theoretical* = 3,300 g/mol and M_n *experimental* = 1700 g/mol).

Within the series of catalysts, **MgCo** is clearly the most highly active and increasing the reaction temperature results in a significant rate enhancement from 455 h^{-1} (80 °C) to 1205 h^{-1} (120 °C) without any compromise in the quality of the polymer produced (Table 1). Comparing the activity of all three catalysts under identical conditions reveals that **MgCo** (1205 h^{-1}) is significantly more active than either **CoCo** (712 h^{-1}) or **MgMg** (368 h^{-1}). It is also >4 times faster than the previously most active heterodinuclear **ZnMg** catalyst featuring the same ancillary ligand (Table 1).[42] In comparison to other leading catalysts in this field, **MgCo** shows a very high activity (Table 1, Supplementary Fig. 7 shows the structures of the literature catalysts).[6,7] For example, compared to a recently reported first example of an In(III) catalyst, **MgCo** is thirty times more active.[43] It is three times more active than a dizinc complex coordinated by a prolinol derivative,[44] and

approximately twice the activity of a tetranuclear La_3Zn catalyst.[45] It is also qualitatively faster than optimized Co(III) catalysts featuring ligand tethered ionic co-catalysts, although direct comparisons may be hindered by the thermal instability of some Co(III) complexes.[46]

Polymerization Kinetics and Chain Shuttling Mechanism

To better understand the enhanced activity, the catalytic rate law and rate-determining step (RDS) were investigated. Polymerization conversion vs. time data were acquired using *in-situ* infrared spectroscopy (Supplementary Fig. 8), by analysing the increase in the absorption intensity corresponding to the formation of PCHC. A range of different **MgCo** concentrations were evaluated, from 0.43 – 1.67 mM, using a 3.33 M concentration of epoxide (CHO) dissolved in diethyl carbonate (DEC) and by applying 1 bar CO_2 pressure, at 100 °C. Plots of epoxide concentration vs. normalized time, using the method described by Bures,[47] showed the best fits for a first order dependence in catalyst concentration (Fig. 2d). Alternative fits for higher or lower orders in catalyst concentration were poor, substantiating the first order assignment (Supplementary Fig. 9). To determine the order in epoxide its concentration was varied from 1– 5 M, in DEC using a concentration of catalyst of 1.67 mM, at 1 bar CO_2 pressure, 100 °C. Semi-logarithmic plots of epoxide concentration vs. time (ln[CHO] vs. time) from 5 – 75 % epoxide conversion (i.e. an integrated rate approach) showed linear fits indicative of a first order dependence on epoxide concentration (Fig. 2e, Supplementary Fig. 10). The dependence on carbon dioxide pressure was determined from 10 – 40 bar, using a catalyst concentration of 1.67 mM, a CHO concentration of 3.33 M in DEC, at 100 °C (Fig. 2f). Plots of activity (TOF) vs. time, where activity is determined as the initial rate from 5 – 15 % monomer conversion, showed a zero order dependence on CO_2 pressure. The

slight reduction in rate at higher CO_2 pressure is in line with previous observations and is probably due to sub-critical CO_2 gas expansion reducing the overall epoxide and catalyst concentrations.[48] Overall the kinetic data are consistent with the homodinuclear catalysts,[42,49,50] and show a rate law dependent to the first order in catalyst and epoxide concentration and independent of carbon dioxide pressure (10-40 bar).

The rate law is rationalized by a chain shuttling mechanistic hypothesis,[8,51] whereby the rate limiting step involves metal carbonate attack at the second metal coordinated epoxide. The polymer chain 'shuttles' between the two metals twice per complete cycle of insertions, i.e. it changes the metal at which it is anionically coordinated (X-type ligand) when the epoxide is inserted and again when CO_2 is inserted.[49] The catalyst features two carboxylate groups but it is proposed that these have different roles in the cycle: one group initiates polymerization but the other remains κ_2 coordinated at the metals.[49]

This bridging carboxylate ligand is proposed to facilitate chain shuttling by changing its site of formal anionic coordination to counter-balance charge as the polymer chain moves (Fig. 3a, Supplementary Fig. 11).[49]

To investigate the chain shuttling process in more detail, the temperature dependence of the rate was investigated from 60 – 125 °C, at 1 bar CO_2 pressure (Supplementary Table 3). The rate of polymerization increases with temperature up to 100 °C, but at higher temperatures polymer (PCHC) formation sharply decreases (Fig. 3b). Concurrently the rate of trans-cyclic carbonate (1825 cm^{-1})[52] formation rapidly increases as observed by IR spectroscopy. There is no observable cis-cyclic carbonate (1804 cm^{-1})[52] by IR spectroscopy. The loss of selectivity at high temperatures may be rationalized by the decreasing solubility of carbon dioxide (in epoxide), as predicted by Henry's Law.[53] As a result, CO_2 insertion becomes rate-limiting and the catalytic resting state shifts from a

metal-carbonate to a metal-alkoxide intermediate. Under these conditions, forward polymerization requires carbon dioxide and is limited by its low solubility. In contrast, cyclic carbonate forms from the metal alkoxide species undergoing chain back-biting and this process is independent of CO_2. Thus, when using low CO_2 pressures, under static conditions, and at high temperatures the reaction conditions favour the formation of mixtures of polymer and cyclic carbonate causing the reaction selectivity to be compromised. To overcome this limitation and to maintain the best rates of polymerization, reactions were conducted at 20 bar CO_2 pressure so as to compensate for high temperature diffusion and solubility limitations (Fig. 3c, Table 2). Under these conditions, the rate of polymerization shows the expected exponential increase from 60 – 140 °C and the **MgCo** catalyst achieves an activity of 12,462 h^{-1}, whilst maintaining the highest polymer and carbon dioxide selectivity (> 99 %). Under these conditions, the rate limiting step remains as metal carbonate attack and the resting state is the metal-carbonate intermediate. Since this species does not undergo significant back-biting reactions, the selectivity for polymer is maintained and negligible quantities of cyclic carbonate by-product are formed.

Catalysis Scope and Benchmarking

MgCo was also tested using a range of other common epoxides, using 0.05 mol% catalyst concentration, 20 bar CO_2 pressure and 100 °C (Supplementary Table 8). Detailed monomer scoping investigations are necessary in future but the preliminary findings show good activity using cyclopentene oxide (TOF = 214 h^{-1}) and vinyl-cyclohexene oxide (TOF = 2900 h^{-1}) (Supplementary Table 8). Poly(cyclopentene carbonate) is of interest in the context of catalysed depolymerization, or chemical recycling, since it shows potential to reform cyclopentene oxide.[54,55] Vinyl-cyclohexene oxide is of interest for the potential

to apply post-functionalization reactions at the alkene as a means to modify the polymer properties and achieve efficient cross-linking.[56-60] **MgCo** shows no activity using bio-based limonene oxide and, under these conditions, using propene oxide, it catalyzes the formation of propene carbonate (TOF = 5 h^{-1}) (Supplementary Table 8).

Objectively, the **MgCo** activity is very high and comparisons both against homodinuclear combinations and other literature catalysts are warranted (Table 2). The most accurate means to compare catalysts is to compare rate coefficients and this is most easily accomplished for the series of complexes featuring the same ancillary ligand and different metal combinations (Table 1).[42] Since it's already been established that these homodinuclear (**ZnZn**, **MgMg**, **CoCo**) and heterodinuclear (**ZnMg**) catalysts show the same rate law,[27,42,49,50] it is possible to properly compare rate coefficients (k_p) and relative rates (k_{rel}, against the **ZnZn** benchmark). At 80 °C, the **MgCo** complex shows a relative rate which is 85 times greater than **ZnZn**. At 120 °C, the **MgCo** relative rate is >1000 times greater than the **ZnZn** analogue, 5 times greater than **MgMg** and approximately double the recently reported **MgZn**. The rate coefficients also confirm that **MgCo** is significantly more active than either of the homodinuclear analogues (**MgMg** or **CoCo**), for example at 120 °C **MgCo** shows double the rate of **CoCo** and four times the rate of **MgMg**. Polymerization catalysis conducted using an equimolar mixture of **MgMg** and **CoCo** showed an average rate for the two complexes and the value was three times less than that for **MgCo** (Table 2, entry 8). This experiment underscores the importance of isolation of the pure heterodinuclear complex and provides good evidence of a synergic interaction between the Mg and Co(II) metals. It also shows there is not any appreciable conversion of the homodinuclear complexes to the **MgCo** species under the conditions of the catalysis.[25,42]

Comparisons with literature catalysts, often tested using higher CO_2 pressure regimes, are more complex since the rate laws and associated rate coefficients are rarely reported. A recently reported homogeneous Fe(III) catalyst (see Supplementary Fig. 12 for catalyst structure), in combination with an ammonium chloride co-catalyst, is around twenty times slower than **MgCo**.[61] Comparing point activity data (TOF values) reveals qualitatively similar, or somewhat higher rates, for **MgCo** compared with the well-known highly active Co(III)-salen/PPNX bicomponent catalyst systems or with trialkyl borane and PPNX catalyst systems.[62-64]

Given the outstanding performance of the catalyst and that the previously most active systems comprised Co(III) complexes, it is relevant to understand whether any appreciable Co(II) oxidation occurs during catalysis. It should be noted that such oxidation is not anticipated from the previous Co(III) salen catalytic literature, which has rather shown thermally induced reduction side-reactions to form inactive Co(II) complexes at high-temperatures.[65] Notwithstanding this prior result, several attempts were made to oxidise the **MgCo(II)** catalyst but all reactions were unsuccessful and resulted in substantial complex decomposition (Supplementary Fig. 13). Cyclic voltammetry experiments using **MgCo(II)** confirm the instability of the MgCo(III) intermediate, with no clear reduction potential being observed (Supplementary Fig. 5). In contrast, the **Co(II)Co(II)** analogue shows two clear oxidations (to Co(II)Co(III) and Co(III)Co(III), respectively) and the concomitant two reduction reactions. The findings using **CoCo** confirm that the heterodinuclear complex **MgCo(II)** is expected to be stable with respect to oxidation and that there is not expected to be any substantial formation of **MgCo(III)** species during catalysis.

Heterodinuclear Synergy

To gain further insight into the metal-metal synergy, the transition state Gibbs free energy ($\Delta G^{‡}$) was determined by an analysis of the temperature dependence of the rate coefficient (Fig. 4a). Experiments were conducted using an initial concentration of epoxide of 3.33 M in DEC, with a catalyst concentration of 1.67 mM, under 20 bar CO_2 pressure and temperatures were varied in 20 °C increments from 60 – 120 °C (Supplementary Fig. 14, Supplementary Tables 4-6). Plots of ln(k/T) vs. 1/T enabled determine of both the transition state enthalpy ($\Delta H^{‡}$) and entropy ($\Delta S^{‡}$) (Supplementary Fig. 15, Supplementary Table 7). The transition state Gibbs free energy ($\Delta G^{‡}$, T = 373 K) values are 94.5 ± 1.2, 97.3 ± 1.5 and 100.2 ± 1.3 kJ mol^{-1} for **MgCo**, **CoCo** and **MgMg**, respectively. Over the series of catalysts, the transition state barrier decreases by 5.7 kJ mol^{-1} which correlates well with the observed 8-fold increase in rate for the heterodinuclear catalyst **MgCo**. The analogous dizinc catalyst (**ZnZn**) shows $\Delta G^{‡}$ = 107 kJ mol^{-1} (T = 373 K)[49,50] and accordingly **MgCo** is ~85-times faster; these findings clearly demonstrate the benefit of targeting the right metal combinations and synergies. The transition state entropy ($\Delta S^{‡}$) is significantly reduced for catalysts containing Mg(II), with values for **MgMg** and **MgCo** catalysts at -45.4 ± 3.7 and -46.1 ± 3.4 J mol^{-1}, respectively, compared to the **CoCo** analogue, -60.2 ± 4.2 J mol^{-1}. (Fig. 4b, Supplementary Table 7). The entropic benefit of using Mg(II) may arise from its low bond directionality which may increase the degrees of freedom (rotational and/or conformational) associated with epoxide coordination. It could also relate to the higher oxophilicity of magnesium (Θ= 0.6) compared to cobalt (Θ= 0.4), as quantified in a recent evaluation of oxophilicity values across the periodic table.[66] The transition state thermodynamic data also show that catalysts containing Co(II) show reduced enthalpy barriers, e.g. $\Delta H^{‡}$ = 77.3 ± 1.2 kJ mol^{-1} for **MgCo** vs. 83.3 ± 1.3 kJ mol^{-1} for **MgMg**, T = 373 K). This finding is in-line with the Co(II)-carbonate being significantly more nucleophilic than its Mg(II) counterpart. Taken

together these experimental data can be interpreted as rationalizing the synergy of the **MgCo** complex since it combines the favourable entropy of epoxide coordination at Mg(II), with a highly nucleophilic Co(II)-carbonate (Fig. 4d, Supplementary Fig. 11). The high lability of Co(II)-carbonates was previously observed in literature describing the formation of cyclic carbonates.[29,30] The ability to replace a Co(II) centre with Mg(II) to accelerate activity is both fundamentally interesting but also practically useful due to its abundance, light-weight and lack of toxicity.[67] Overall, the enhanced performance for the heterodinuclear **MgCo** catalyst unambiguously arises from synergic interaction between the metals and kinetic analysis signals that the barrier to the rate limiting step is reduced by using the Mg(II) to carry out epoxide coordination and the Co(II) centre to provide the reactive (nucleophilic) carbonate group to attack and ring-open the epoxide (Supplementary Fig. 11).

These results provide a new strategy for the design, preparation and understanding of highly efficient, selective, stable and inexpensive catalysts for CO_2 copolymerization.

The kinetic and mechanistic findings clearly signal some future directions to improve other catalysts' performances and to design new catalysts for these processes. Most clearly, there is a route to improve existing dinucleating □-diiminate and salen catalysts by targeting heterodinuclear complexes, exploiting the thermodynamic stability demonstrated in this work and by using Mg(II) in place of Zn(II)/Co(II/III)/Cr(III).[68-70] Such heterodinuclear MgCo(II/III), MgCr(II/III) complexes would have the added benefit of replacing 50% of the expensive, coloured and heavy transition metal with Mg(II). There is also potential to exploit main-group/transition metal synergy in other CO_2 utilizations, for example di-Co(II) complexes are highly active photoredox catalysts for transforming CO_2 into CO;[71-73] very recently a Co(II)/Zn(II) complex showed yet higher activity.[71] CO_2

terpolymerizations and switchable catalytic processes are currently limited by low catalyst activities and so better catalysts should allow access to a broader range of CO_2 containing materials and properties.[74-78] Beyond the field of CO_2 utilization, there is increasing interest in main group/Co(II) heterodinuclear catalysts, relevant to those explored in this work, for processes including nitrogen activation,[79-81] electrophilic amination,[82] CH and CF activation processes.[83,84]

Conclusions

A synergic and highly active heterodinuclear **MgCo** complex for epoxide/CO_2 copolymerization was synthesized in high yield by a one-pot, thermodynamically controlled reaction. It was characterized using a range of techniques, including XPS, mass spectrometry, magnetometry and cyclic voltammetry. The **MgCo** catalyst achieves very high activity at either 1 bar CO_2 pressure (TOF = 1205 h^{-1}) or at 20 bar pressure (TOF = 12,400 h^{-1}) and produces perfectly alternating copolymer for CO_2/CHO coupling and was found active for other epoxide monomers including vCHO, CPO and PO (Supplementary Table 8). Detailed kinetic studies reveal the synergy arises because the magnesium centre enhances the transition state entropy, through epoxide coordination, and cobalt reduces the transition state enthalpy, by the greater nucleophilicity of the cobalt-carbonate. This catalyst highlights the potential for heterodinuclear synergy and underscores the importance of metal selection according to its specific role in the cycle. The findings are expected to be broadly applicable to other homodinuclear polymerization and switchable catalysts. Generally, the work provides a rationale and understanding of how to exploit synergic interactions in homogeneous catalysis.

Acknowledgements

The EPSRC (EP/L017393/1, EP/K014668/1) and EIT Climate KIC (EnCO_2re) are acknowledged for research funding. AD acknowledges a DTP studentship, co-funded by Econic technologies, for financial support. AR acknowledges the support of Imperial College for her Imperials College Research Fellowship.

Author Contributions

AD and CW conceived the project. AD designed and performed the synthetic experiments. SK designed and performed the CV and SQUID experiments. AR designed and performed the XPS study. AD and CW prepared the manuscript.

Conflict of Interest

CW is a director of econic technologies.

Data Availability

All the data supporting the findings of this study are available within the paper and its supplementary information files or from the corresponding author on request

References

1 Artz, J. *et al.* Sustainable Conversion of Carbon Dioxide: An Integrated Review of Catalysis and Life Cycle Assessment. *Chem. Rev.* **118**, 434-504, (2018).
2 Zhang, X. Y., Fevre, M., Jones, G. O. & Waymouth, R. M. Catalysis as an Enabling Science for Sustainable Polymers. *Chem. Rev.* **118**, 839-885, (2018).
3 Kleij, A. W., North, M. & Urakawa, A. CO_2 Catalysis. *ChemSusChem* **10**, 1036-1038, (2017).
4 Zhu, Y., Romain, C. & Williams, C. K. Sustainable polymers from renewable resources. *Nature* **540**, 354-362, (2016).
5 Wang, Y. Y. & Darensbourg, D. J. Carbon dioxide-based functional polycarbonates: Metal catalyzed copolymerization of CO_2 and epoxides. *Coord. Chem. Rev.* **372**, 85-100, (2018).
6 Kozak, C. M., Ambrose, K. & Anderson, T. S. Copolymerization of carbon dioxide and epoxides by metal coordination complexes. *Coord. Chem. Rev.* **376**, 565-587, (2018).
7 Garden, J. A. Exploiting multimetallic catalysts to access polymer materials from CO_2. *Green Mater.* **5**, 103-108, (2017).
8 Trott, G., Saini, P. K. & Williams, C. K. Catalysts for CO_2/epoxide ring-opening copolymerization. *Philos. Trans. R. Soc. A-Math. Phys. Eng. Sci.* **374**, 19, (2016).

9 Assen, N. v. d. & Bardow, A. Life cycle assessment of polyols for polyurethane production using CO_2 as feedstock: insights from an industrial case study. *Green Chem.* **16**, 3272-3280, (2014).
10 Chapman, A. M., Keyworth, C., Kember, M. R., Lennox, A. J. J. & Williams, C. K. Adding Value to Power Station Captured CO_2: Tolerant Zn and Mg Homogeneous Catalysts for Polycarbonate Polyol Production. *ACS Catal.* **5**, 1581-1588, (2015).
11 Scharfenberg, M., Hilf, J. & Frey, H. Functional Polycarbonates from Carbon Dioxide and Tailored Epoxide Monomers: Degradable Materials and Their Application Potential. *Adv. Funct. Mater.* **28**, 16, (2018).
12 Stoesser, T. *et al.* Bio-derived polymers for coating applications: comparing poly(limonene carbonate) and poly(cyclohexadiene carbonate). *Polym. Chem.* **8**, 6099-6105, (2017).
13 Subhani, M. A., Kohler, B., Gurtler, C., Leitner, W. & Muller, T. E. Transparent Films from CO_2-Based Polyunsaturated Poly(ether carbonate)s: A Novel Synthesis Strategy and Fast Curing. *Angew. Chem.-Int. Edit.* **55**, 5591-5596, (2016).
14 Li, C., Sablong, R. J. & Koning, C. E. Chemoselective Alternating Copolymerization of Limonene Dioxide and Carbon Dioxide: A New Highly Functional Aliphatic Epoxy Polycarbonate. *Angew. Chem.-Int. Edit.* **55**, 11572-11576, (2016).
15 Luinstra, G. A. Poly(Propylene Carbonate), Old Copolymers of Propylene Oxide and Carbon Dioxide with New Interests: Catalysis and Material Properties. *Polym. Rev.* **48**, 192-219, (2008).
16 Hauenstein, O., Reiter, M., Agarwal, S., Rieger, B. & Greiner, A. Bio-based polycarbonate from limonene oxide and CO_2 with high molecular weight, excellent thermal resistance, hardness and transparency. *Green Chem.* **18**, 760-770, (2016).
17 Hauenstein, O., Agarwal, S. & Greiner, A. Bio-based polycarbonate as synthetic toolbox. *Nat. Commun.* **7**, 11862, (2016).
18 Romain, C., Thevenon, A., Saini, P. K. & Williams, C. K. in *Carbon Dioxide and Organometallics* Vol. 53 *Topics in Organometallic Chemistry* (ed X. B. Lu) 101-141 (2016).
19 Kremer, A. B. & Mehrkhodavandi, P. Dinuclear catalysts for the ring opening polymerization of lactide. *Coord. Chem. Rev.* **380**, 35-57, (2019).
20 Wang, P. K. *et al.* Breaking scaling relations to achieve low-temperature ammonia synthesis through LiH-mediated nitrogen transfer and hydrogenation. *Nat. Chem.* **9**, 64-70, (2017).
21 Kattel, S., Ramirez, P. J., Chen, J. G., Rodriguez, J. A. & Liu, P. Active sites for CO_2 hydrogenation to methanol on Cu/ZnO catalysts. *Science* **355**, 1296-1299, (2017).
22 Chen, Y. Z. *et al.* Multifunctional PdAg@MIL-101 for One-Pot Cascade Reactions: Combination of Host-Guest Cooperation and Bimetallic Synergy in Catalysis. *ACS Catal.* **5**, 2062-2069, (2015).
23 Powers, D. C. & Ritter, T. Bimetallic Redox Synergy in Oxidative Palladium Catalysis. *Acc. Chem. Res.* **45**, 840-850, (2012).
24 Garden, J. A., Saini, P. K. & Williams, C. K. Greater than the Sum of Its Parts: A Heterodinuclear Polymerization Catalyst. *J. Am. Chem. Soc.* **137**, 15078-15081, (2015).
25 Deacy, A. C., Durr, C. B., Garden, J. A., White, A. J. P. & Williams, C. K. Groups 1, 2 and Zn(II) Heterodinuclear Catalysts for Epoxide/CO_2 Ring-Opening Copolymerization. *Inorg. Chem.* **57**, 15575-15583, (2018).
26 Deacy, A. C., Durr, C. B. & Williams, C. K. Heterodinuclear complexes featuring Zn(ii) and M = Al(iii), Ga(iii) or In(iii) for cyclohexene oxide and CO_2 copolymerisation. *Dalton Transactions* **49**, 223-231, (2020).

27 Kember, M. R., Jutz, F., Buchard, A., White, A. J. P. & Williams, C. K. Di-cobalt(ii) catalysts for the copolymerisation of CO_2 and cyclohexene oxide: support for a dinuclear mechanism? *Chem. Sci.* **3**, 1245-1255, (2012).
28 Kember, M. R., White, A. J. P. & Williams, C. K. Highly Active Di- and Trimetallic Cobalt Catalysts for the Copolymerization of CHO and CO_2 at Atmospheric Pressure. *Macromolecules* **43**, 2291-2298, (2010).
29 Darensbourg, D. J. & Moncada, A. I. (Salen)Co(II)/n-Bu_4NX Catalysts for the Coupling of CO_2 and Oxetane: Selectivity for Cyclic Carbonate Formation in the Production of Poly-(trimethylene carbonate). *Macromolecules* **42**, 4063-4070, (2009).
30 Darensbourg, D. J. Making Plastics from Carbon Dioxide: Salen Metal Complexes as Catalysts for the Production of Polycarbonates from Epoxides and CO_2. *Chem. Rev.* **107**, 2388-2410, (2007).
31 Shen, Y.-M., Duan, W.-L. & Shi, M. Chemical Fixation of Carbon Dioxide Catalyzed by Binaphthyldiamino Zn, Cu, and Co Salen-Type Complexes. *J. Org. Chem.* **68**, 1559-1562, (2003).
32 Ohkawara, T., Suzuki, K., Nakano, K., Mori, S. & Nozaki, K. Facile Estimation of Catalytic Activity and Selectivities in Copolymerization of Propylene Oxide with Carbon Dioxide Mediated by Metal Complexes with Planar Tetradentate Ligand. *J. Am. Chem. Soc.* **136**, 10728-10735, (2014).
33 Liu, Y., Ren, W. M., Zhang, W. P., Zhao, R. R. & Lu, X. B. Crystalline CO_2-based polycarbonates prepared from racemic catalyst through intramolecularly interlocked assembly. *Nat. Commun.* **6**, (2015).
34 Na, S. J. *et al.* Elucidation of the Structure of a Highly Active Catalytic System for CO_2/Epoxide Copolymerization: A salen-Cobaltate Complex of an Unusual Binding Mode. *Inorg. Chem.* **48**, 10455-10465, (2009).
35 Darensbourg, D. J. & Yeung, A. D. A concise review of computational studies of the carbon dioxide–epoxide copolymerization reactions. *Polym. Chem.* **5**, 3949-3962, (2014).
36 Kember, M. R. & Williams, C. K. Efficient Magnesium Catalysts for the Copolymerization of Epoxides and CO_2; Using Water to Synthesize Polycarbonate Polyols. *J. Am. Chem. Soc.* **134**, 15676-15679, (2012).
37 Mishra, V., Lloret, F. & Mukherjee, R. Coordination versatility of 1,3-bis[3-(2-pyridyl)pyrazol-1-yl]propane: Co(II) and Ni(II) complexes. *Inorg. Chim. Acta* **359**, 4053-4062, (2006).
38 Du, K., Thorarinsdottir, A. E. & Harris, T. D. Selective Binding and Quantitation of Calcium with a Cobalt-Based Magnetic Resonance Probe. *J. Am. Chem. Soc.* **141**, 7163-7172, (2019).
39 Halfen, J. A. *et al.* Synthetic Models of the Inactive Copper(II)−Tyrosinate and Active Copper(II)−Tyrosyl Radical Forms of Galactose and Glyoxal Oxidases. *J. Am. Chem. Soc.* **119**, 8217-8227, (1997).
40 Itoh, S. *et al.* Model Complexes for the Active Form of Galactose Oxidase. Physicochemical Properties of Cu(II)− and Zn(II)−Phenoxyl Radical Complexes. *Inorg. Chem.* **39**, 3708-3711, (2000).
41 DiCiccio, A. M., Longo, J. M., Rodríguez-Calero, G. G. & Coates, G. W. Development of Highly Active and Regioselective Catalysts for the Copolymerization of Epoxides with Cyclic Anhydrides: An Unanticipated Effect of Electronic Variation. *J. Am. Chem. Soc.* **138**, 7107-7113, (2016).
42 Trott, G., Garden, J. A. & Williams, C. K. Heterodinuclear zinc and magnesium catalysts for epoxide/CO_2 ring opening copolymerizations. *Chem. Sci.* **10**, 4618-4627, (2019).

43 Thevenon, A. *et al.* Indium Catalysts for Low-Pressure CO_2/Epoxide Ring-Opening Copolymerization: Evidence for a Mononuclear Mechanism? *J. Am. Chem. Soc.* **140**, 6893–6903, (2018).
44 Schutze, M., Dechert, S. & Meyer, F. Highly Active and Readily Accessible Proline-Based Dizinc Catalyst for CO_2/Epoxide Copolymerization. *Chem.-Eur. J.* **23**, 16472-16475, (2017).
45 Nagae, H. *et al.* Lanthanide Complexes Supported by a Trizinc Crown Ether as Catalysts for Alternating Copolymerization of Epoxide and CO_2: Telomerization Controlled by Carboxylate Anions. *Angew. Chem.-Int. Edit.* **57**, 2492-2496, (2018).
46 Ren, W.-M. *et al.* Highly Active, Bifunctional Co(III)-Salen Catalyst for Alternating Copolymerization of CO_2 with Cyclohexene Oxide and Terpolymerization with Aliphatic Epoxides. *Macromolecules* **43**, 1396, (2010).
47 Burés, J. A Simple Graphical Method to Determine the Order in Catalyst. *Angew. Chem.-Int. Edit.* **55**, 2028-2031, (2016).
48 Mang, S., Cooper, A. I., Colclough, M. E., Chauhan, N. & Holmes, A. B. Copolymerization of CO_2 and 1,2-Cyclohexene Oxide Using a CO_2-Soluble Chromium Porphyrin Catalyst. *Macromolecules* **33**, 303-308, (2000).
49 Buchard, A. *et al.* Experimental and Computational Investigation of the Mechanism of Carbon Dioxide/Cyclohexene Oxide Copolymerization Using a Dizinc Catalyst. *Macromolecules* **45**, 6781-6795, (2012).
50 Jutz, F., Buchard, A., Kember, M. R., Fredrickson, S. B. & Williams, C. K. Mechanistic Investigation and Reaction Kinetics of the Low-Pressure Copolymerization of Cyclohexene Oxide and Carbon Dioxide Catalyzed by a Dizinc Complex. *J. Am. Chem. Soc.* **133**, 17395–17405, (2011).
51 Saini, P. K., Romain, C. & Williams, C. K. Dinuclear metal catalysts: improved performance of heterodinuclear mixed catalysts for CO_2–epoxide copolymerization. *Chem. Commun.* **50**, 4164-4167, (2014).
52 Buchard, A., Kember, M. R., Sandeman, K. G. & Williams, C. K. A bimetallic iron(iii) catalyst for CO_2/epoxide coupling. *Chem. Commun.* **47**, 212-214, (2011).
53 Gui, X., Tang, Z. G. & Fei, W. Y. Solubility of CO_2 in Alcohols, Glycols, Ethers, and Ketones at High Pressures from (288.15 to 318.15) K. *J. Chem. Eng. Data* **56**, 2420-2429, (2011).
54 Darensbourg, D. J., Wei, S.-H., Yeung, A. D. & Ellis, W. C. An Efficient Method of Depolymerization of Poly(cyclopentene carbonate) to Its Comonomers: Cyclopentene Oxide and Carbon Dioxide. *Macromolecules* **46**, 5850-5855, (2013).
55 Lu, X.-B., Liu, Y. & Zhou, H. Learning Nature: Recyclable Monomers and Polymers. *Chem.-Eur. J.* **24**, 11255-11266, (2018).
56 Darensbourg, D. J. & Wang, Y. Y. Terpolymerization of propylene oxide and vinyl oxides with CO_2: copolymer cross-linking and surface modification via thiol-ene click chemistry. *Polym. Chem.* **6**, 1768-1776, (2015).
57 Darensbourg, D. J., Chung, W. C., Arp, C. J., Tsai, F. T. & Kyran, S. J. Copolymerization and Cycloaddition Products Derived from Coupling Reactions of 1,2-Epoxy-4-cyclohexene and Carbon Dioxide. Postpolymerization Functionalization via Thiol-Ene Click Reactions. *Macromolecules* **47**, 7347-7353, (2014).
58 Geschwind, J., Wurm, F. & Frey, H. From CO_2-Based Multifunctional Polycarbonates With a Controlled Number of Functional Groups to Graft Polymers. *Macromol. Chem. Phys.* **214**, 892-901, (2013).
59 Yang, G.-W. & Wu, G.-P. High-Efficiency Construction of CO_2-Based Healable Thermoplastic Elastomers via a Tandem Synthetic Strategy. *ACS Sust. Chem. Eng.* **7**, 1372-1380, (2019).

60 Yi, N., Chen, T. T. D., Unruangsri, J., Zhu, Y. & Williams, C. K. Orthogonal functionalization of alternating polyesters: selective patterning of (AB)n sequences. *Chem. Sci.* **10**, 9974-9980, (2019).
61 Della Monica, F. *et al.* [OSSO]-Type Iron(III) Complexes for the Low-Pressure Reaction of Carbon Dioxide with Epoxides: Catalytic Activity, Reaction Kinetics, and Computational Study. *ACS Catal.* **8**, 6882-6893, (2018).
62 Zhang, D., Boopathi, S. K., Hadjichristidis, N., Gnanou, Y. & Feng, X. Metal-Free Alternating Copolymerization of CO_2 with Epoxides: Fulfilling "Green" Synthesis and Activity. *J. Am. Chem. Soc.* **138**, 11117-11120, (2016).
63 Darensbourg, D. J., Mackiewicz, R. M. & Billodeaux, D. R. Pressure Dependence of the Carbon Dioxide/Cyclohexene Oxide Coupling Reaction Catalyzed by Chromium Salen Complexes. Optimization of the Comonomer-Alternating Enchainment Pathway. *Organometallics* **24**, 144, (2005).
64 Liu, Y., Ren, W.-M., Liu, J. & Lu, X.-B. Asymmetric Copolymerization of CO_2 with meso-Epoxides Mediated by Dinuclear Cobalt(III) Complexes: Unprecedented Enantioselectivity and Activity. *Angew. Chem.-Int. Edit.* **52**, 11594-11598, (2013).
65 Ren, W.-M., Liu, Z.-W., Wen, Y.-Q., Zhang, R. & Lu, X.-B. Mechanistic Aspects of the Copolymerization of CO_2 with Epoxides Using a Thermally Stable Single-Site Cobalt(III) Catalyst. *J. Am. Chem. Soc.* **131**, 11509-11518, (2009).
66 Kepp, K. P. A Quantitative Scale of Oxophilicity and Thiophilicity. *Inorg. Chem.* **55**, 9461-9470, (2016).
67 Hill, M. S., Liptrot, D. J. & Weetman, C. Alkaline earths as main group reagents in molecular catalysis. *Chem. Soc. Rev.* **45**, 972-988, (2016).
68 Reiter, M., Vagin, S., Kronast, A., Jandl, C. & Rieger, B. A Lewis acid [small beta]-diiminato-zinc-complex as all-rounder for co- and terpolymerisation of various epoxides with carbon dioxide. *Chem. Sci.* **8**, 1876-1882, (2017).
69 Liu, Y., Ren, W.-M., He, K.-K. & Lu, X.-B. Crystalline-gradient polycarbonates prepared from enantioselective terpolymerization of meso-epoxides with CO_2. *Nat. Commun.* **5**, 5687-5694, (2014).
70 Nakano, K., Hashimoto, S. & Nozaki, K. Bimetallic mechanism operating in the copolymerization of propylene oxide with carbon dioxide catalyzed by cobalt–salen complexes. *Chem. Sci.* **1**, 369-373, (2010).
71 Ouyang, T. *et al.* Dinuclear Metal Synergistic Catalysis Boosts Photochemical CO_2-to-CO Conversion. *Angew. Chem.-Int. Edit.* **57**, 16480-16485, (2018).
72 Ouyang, T., Huang, H. H., Wang, J. W., Zhong, D. C. & Lu, T. B. A Dinuclear Cobalt Cryptate as a Homogeneous Photocatalyst for Highly Selective and Efficient Visible-Light Driven CO_2 Reduction to CO in CH_3CN/H_2O Solution. *Angew. Chem.-Int. Edit.* **56**, 738-743, (2017).
73 Hogue, R. W., Schott, O., Hanan, G. S. & Brooker, S. A Smorgasbord of 17 Cobalt Complexes Active for Photocatalytic Hydrogen Evolution. *Chem.-Eur. J.* **24**, 9820-9832, (2018).
74 Romain, C. *et al.* Chemoselective Polymerizations from Mixtures of Epoxide, Lactone, Anhydride, and Carbon Dioxide. *J. Am. Chem. Soc.* **138**, 4120-4131, (2016).
75 Chen, T. T. D., Zhu, Y. & Williams, C. K. Pentablock Copolymer from Tetracomponent Monomer Mixture Using a Switchable Dizinc Catalyst. *Macromolecules* **51**, 5346-5351, (2018).
76 Stößer, T. & Williams, C. K. Selective Polymerization Catalysis from Monomer Mixtures: Using a Commercial Cr-Salen Catalyst To Access ABA Block Polyesters. *Angew. Chem.-Int. Edit.* **57**, 6337-6341, (2018).

77 Stößer, T., Mulryan, D. & Williams, C. K. Switch Catalysis To Deliver Multi-Block Polyesters from Mixtures of Propene Oxide, Lactide, and Phthalic Anhydride. *Angew. Chem.-Int. Edit.* **57**, 16893-16897, (2018).
78 Stößer, T., Chen, T. T. D., Zhu, Y. & Williams, C. K. 'Switch' catalysis: from monomer mixtures to sequence-controlled block copolymers. *Phil. Trans. R. Soc. A* **376**, 20170066, (2018).
79 Siedschlag, R. B. *et al.* Catalytic Silylation of Dinitrogen with a Dicobalt Complex. *J. Am. Chem. Soc.* **137**, 4638-4641, (2015).
80 Wu, B., Gramigna, K. M., Bezpalko, M. W., Foxman, B. M. & Thomas, C. M. Heterobimetallic Ti/Co Complexes That Promote Catalytic N–N Bond Cleavage. *Inorg. Chem.* **54**, 10909-10917, (2015).
81 Dugan, T. R., MacLeod, K. C., Brennessel, W. W. & Holland, P. L. Cobalt–Magnesium and Iron–Magnesium Complexes with Weakened Dinitrogen Bridges. *Eur. J. Inorg. Chem.* **2013**, 3891-3897, (2013).
82 Li, J. *et al.* Cobalt-Catalyzed Electrophilic Aminations with Anthranils: An Expedient Route to Condensed Quinolines. *J. Am. Chem. Soc.* **141**, 98-103, (2019).
83 Mei, R., Sauermann, N., Oliveira, J. C. A. & Ackermann, L. Electroremovable Traceless Hydrazides for Cobalt-Catalyzed Electro-Oxidative C–H/N–H Activation with Internal Alkynes. *J. Am. Chem. Soc.* **140**, 7913-7921, (2018).
84 Bakewell, C., Ward, B. J., White, A. J. P. & Crimmin, M. R. A combined experimental and computational study on the reaction of fluoroarenes with Mg–Mg, Mg–Zn, Mg–Al and Al–Zn bonds. *Chem. Sci.* **9**, 2348-2356, (2018).

List Of Figure Captions:

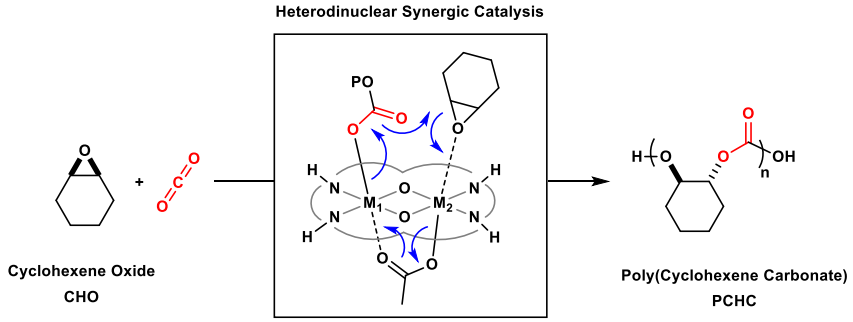

Figure 1: The ring opening copolymerization (ROCOP) of cyclohexene oxide and carbon dioxide, catalysed by heterodinuclear synergic metal catalysts (the proposed rate limiting step is illustrated, where M_1, M_2 are the two metals and OP represents the growing polymer chain, grey loops represent the ligand backbone).

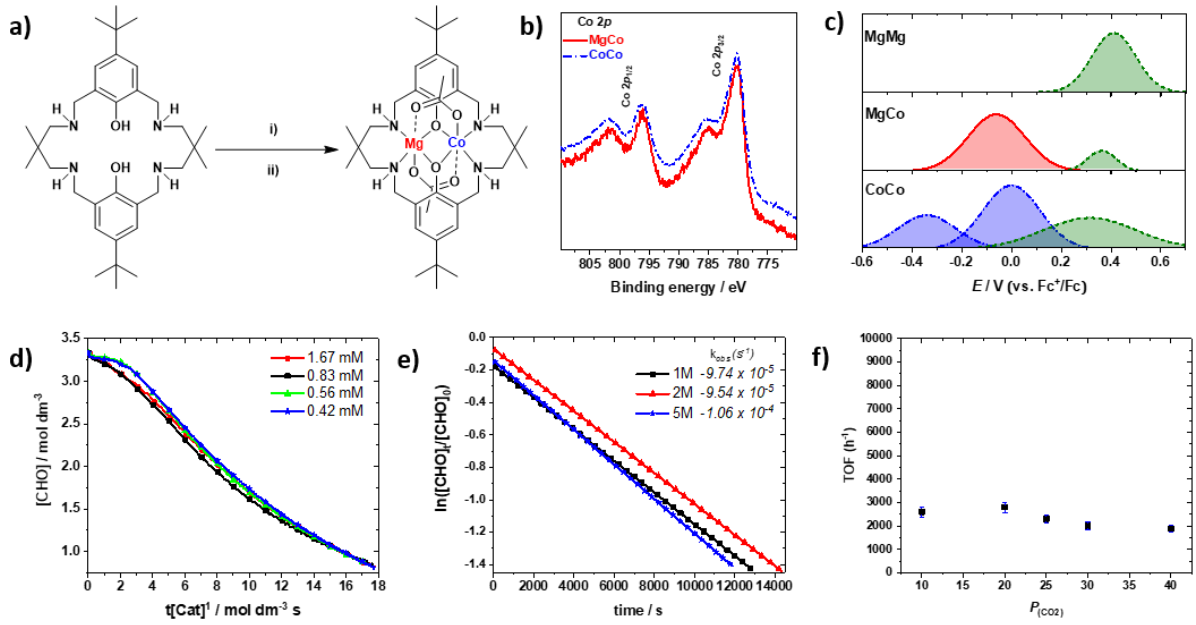

Figure 2: Preparation, characterization and polymerization kinetics of the **MgCo** catalyst. a) Illustration of the route to prepare the heterodinuclear **MgCo** catalyst. Reagents and conditions: i) $Mg\{N(Si(CH_3)_3)_2\}_2$, THF, 25 °C, 1 h. ii) $Co(OAc)_2$, THF, 100 °C, 16 h, 78 %. b) X-ray Photoelectron spectroscopy reveals different binding energies (eV) for the $2p_{1/2}$ and $2p_{3/2}$ orbitals of **MgCo** (—) and **CoCo** (–·–) (for further information see Supplementary Fig. 3). c) Cyclic Voltammetry is used to show different redox potentials (E / V) for **MgMg, MgCo** and **CoCo.** The data are obtained vs. Ferrocium$^+$/Ferrocene, in THF, 0.1 M $[^nBu_4N][PF_6]$ and at 100 mV s^{-1} (for full cyclic voltammograms see Supplementary Fig. 5). d) Kinetic data using **MgCo** catalyst for the ring-opening copolymerization of cyclohexene oxide and carbon dioxide (CHO/CO_2 ROCOP). The first order dependence on catalyst concentration is determined from the linear plots of [CHO] vs. t[cat]^x, x = 1. e) The order in epoxide concentration is determined from the linear fit to plots of ln[CHO] vs. time. f) The order in carbon dioxide pressure is determined from plots of initial rate (h^{-1}) vs. pressure of CO_2 (bar), with error bars, from duplicate runs, marked in blue.

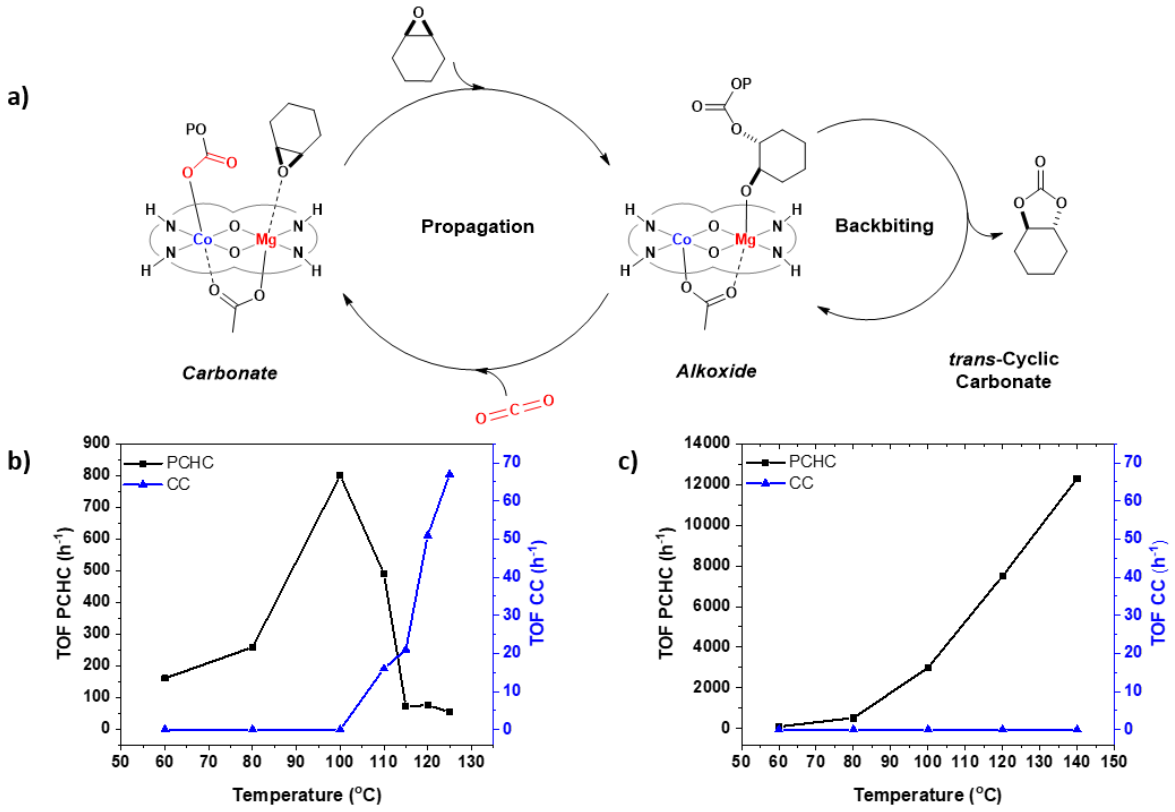

Figure 3: The Chain Shuttling Mechanism for the copolymerization (CHO/CO_2 ROCOP) using **MgCo**. a) Illustration of the Chain Shuttling propagation mechanism, showing the formation of the polycarbonate (PCHC) and side-reactions which occur at higher temperature (low carbon dioxide pressure) to form trans-cyclic carbonate (CC). b) and c) Show the relationship between the catalyst activity (h^{-1}) and temperature (°C) for the formation of polymer (PCHC ■) and cyclic carbonate (CC ▲) at 1 bar pressure of carbon dioxide (b) and the same data but determined at 20 bar CO_2 pressure(c).

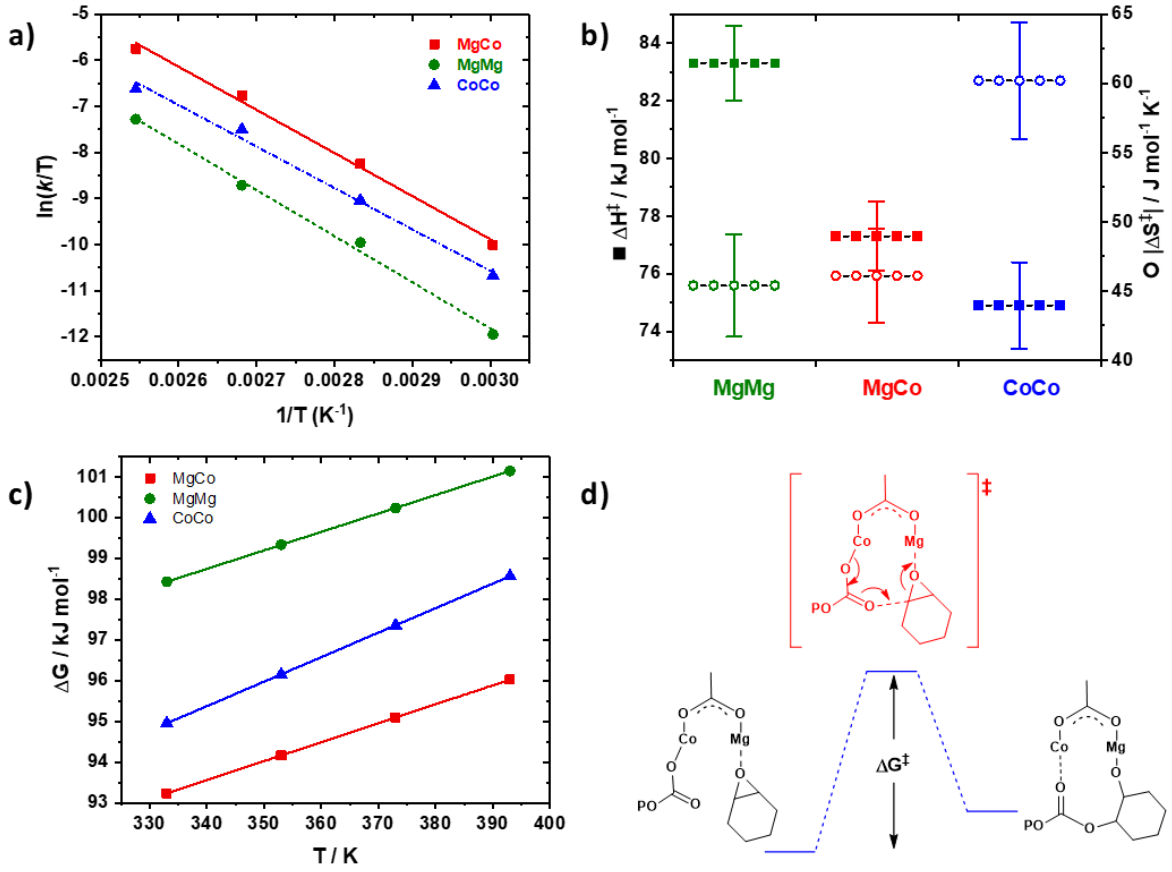

Figure 4: Data providing insight into the factors governing heterodinuclear synergy in polymerization catalysis using kinetic data to compare the **MgCo** heterodinuclear catalyst with homodinuclear analogues **MgMg** and **CoCo**. a) Van't Hoff plots of ln(k/T) vs. 1/T (K^{-1}) for **MgMg** (●) **CoCo** (▲) and **MgCo** (■) over the temperature range 60 – 120 °C, under 20 bar CO_2 pressure. b) The kinetic data allow determination of the transition state enthalpy values, $\Delta H^{‡}$ (■, with errors ±1.3), and entropy values, $\Delta S^{‡}$ (O, with errors ±3.7), for **MgMg**, **CoCo** and **MgCo**. c) The plot shows the variation in the overall transition state Gibbs Free Energy ($\Delta G^{‡}$) vs. temperature (K) for **MgMg** (●, ±1.3) **CoCo** (▲, ±1.5) and **MgCo** (■, ±1.2). The errors are determined using Least Squares Fitting Analysis. d) Illustrates for the rate determining step occurring in the Chain Shuttling Mechanism with the transition state Gibbs Free Energy ($\Delta G^{‡}$) marked (Supplementary Fig. 11 illustrates the reactions occurring during initiation, propagation and termination).

List of Tables:

Table 1: Shows data for the ring-opening copolymerization (ROCOP) of carbon dioxide/cyclohexene oxide (CO_2/CHO) at 1 bar CO_2, using the heterodinuclear catalyst **MgCo** and compared with homodinuclear catalysts, **CoCo** and **MgMg**.[a]

#	Catalyst	T (°C)	Time (min)	CO_2[b]: Polym. (%)[c]	TON[d]	TOF (h^{-1})[e]	M_n [Đ][f] (kg mol^{-1})
1	**MgCo**	80	60	> 99: > 99	455	455 (±15)	1.7 [1.13]
2	**MgCo**	100	40	> 99: > 99	465	699 (±24)	1.6 [1.15]
3	**MgCo**	120	25	> 99 : 99	502	1205 (±41)	2.1 [1.24]
4	**CoCo**	120	60	> 99 : 96	712	712 (±24)	2.5 [1.20]
5	**MgMg**	120	60	> 99 : > 99	368	368 (±13)	1.8 [1.16]

6	**MgZn** *g, 42*	80	360	> 99 : > 99	438	98	12.7[1.04] 5.1 [1.16]
7	**LIn(O^{t}Bu)** *g, 43*	80	2880	> 99 : 95	350	15	3.4 [1.32]
8	**L$_2$Zn$_2$** *g, 44*	80	1440	> 99: 98	1684	149	2.7 [1.28]
9	**LZn$_3$Ce(OAc)$_3$** *h, 45*	100	180	> 99 :> 99	900	300	15.0[1.20]
10	**LCo(X)** *i, 46*	50	300	> 99 : > 99	1315	263	48.2[1.12]

[a]Copolymerization conditions: 0.05 mol % cat loading, 20 equiv. 1,2-cyclohexane diol, 1 bar CO_2, CHO neat (9.99 M). [b]Expressed as a percentage of CO_2 uptake vs the theoretical maximum (100 %), determined by comparison of the relative integrals of the ^{1}H NMR resonances due to carbonate (δ 4.65 ppm) and ether (δ 3.45 ppm) linkages in the polymer backbone. [c]Expressed as a percentage of polymer formation vs. the theoretical maximum (100 %), determined by comparison of the relative integrals of the ^{1}H NMR proton resonances due to polymer (4.65 ppm), cis-cyclic carbonate (4.68 ppm) and trans-cyclic carbonate (4.00 ppm). [d]Turnover number (TON) = number of moles of cyclohexene oxide consumed / number of moles of catalyst. [e]Turnover frequency (ToF) = TON / Time (h). [f]Determined by SEC, in THF, using narrow-M_n polystyrene standards as the calibrant; dispersity is given in brackets. [g] These literature catalysts were tested at 0.1 mol % cat, 1 bar CO_2 for more details see references.[42-44] [h] This literature catalyst was tested at 0.05 mol % cat, 3 bar CO_2.[45] [i] This literature catalyst was tested at 0.02 mol % cat, 1 bar CO_2.[46] For the chemical structures of all the literature catalysts see Supplementary Fig. 7.

Table 2: Shows the data for the ROCOP of CO_2/CHO under 20 bar pressure (CO_2) and variable temperatures using **MgCo** and compared with homodinuclear analogues and other high-performance catalysts from the literature.[a]

#	Cat.	T (°C)	Poly. (%)[b]	TOF (h^{-1})[c]	k_p (x10^3) ($dm^3\ mol^{-1}\ s^{-1}$)[d]	k_{rel}[e]
1	**MgCo**	60	> 99	80 (±2)	15.1 (±0.5)	14
2	**MgCo**	80	> 99	510 (±15)	93.1 (±2.8)	85
3	**MgCo**	100	> 99	3200 (±96)	428.9 (±12.9)	390
4	**MgCo**	120	> 99	7200 (±216)	1231.2 (±36.9)	1120
5	**MgCo**	140	> 99	12460 (±374)	1784.4 (±53.5)	1622
6	**MgMg**	120	> 99	1060 (±11)	269.7 (±8.1)	245
7	**CoCo**	120	> 99	4200 (±126)	559.2 (±16.8)	508
8	**CoCo:MgMg** (50:50)	120	> 99	2400 (±72)	405.0 (±12.2)	368
9	**ZnZn**	80	92	20	11.0	1
10	**MgZn** *f,42*	120	> 99	2400	514.0	467
11	**BEt$_3$/PPNCl** *g, 62*	80	> 99	600	-	-
12	**CrSalen, PPNCl** *h,63*	80	> 99	1153	-	-
13	**LCo$_2$X, PPNX** *i, 64*	25	> 99	1356	-	-
14	**LCo$_2$X** *i, 64*	25	> 99	200	-	-
15	**LFeCl, ^{n}Bu$_4$NCl** *j,61*	80	> 99	400	0.0056	5

*[a]Copolymerization conditions: cat : CHO 0.05 mol %, 20 eq. CHD, 20 bar CO_2. All entries report >99 CO_2 selectivity vs. theoretical maximum (100 %), determined by comparison of the relative integrals of the ^{1}H NMR resonances due to carbonate (δ 4.65 ppm) and ether (δ 3.45 ppm) linkages in the polymer backbone δ 4.65 ppm) and ether (δ 3.45 ppm) linkages in the polymer backbone. Entries 1-8 gone to full conversion (>90 %, >1800 TON) forming polycarbonate polyols of molecular weight 1-3 kg mol^{-1}. [b]Expressed as a percentage of polymer formation vs. the theoretical maximum (100 %), determined by comparison of the relative integrals of the ^{1}H NMR proton resonances due to polymer (4.65 ppm), cis-cyclic carbonate (4.68 ppm) and trans-cyclic carbonate (4.00 ppm). [c]Turnover frequency (TOF) = TON / Time (h) (measured between 5-20 % conversion). [d]$k_p = k_{obs}$ / [cat]^1, k_{obs} determined from the gradient of $ln([CHO]_t/[CHO]_0)$ vs. time plot [cat] = 1.67 mM, over the conversion range 5-75 %. [e]Rate constant relative to **ZnZn** at 80 °C, $k_{rel} = k/0.0011$. [f]0.1 mol% cat, 20 bar CO_2, TON and TOF calculated by raw data supplied by author. [g]0.03mol% cat, 0.015 mol% PPNCl, 10 bar CO_2. [h]0.043 mol %, 35 bar CO_2. [i]0.1 mol % cat, 0.2 mol % PPNCl, 20 bar CO_2. [j]0.1 mol% cat, 0.1mol% ^{n}Bu$_4$N, 10 bar CO_2. For structures of literature catalysts see Supplementary Fig. 12.*

Graphic Abstract/TOC

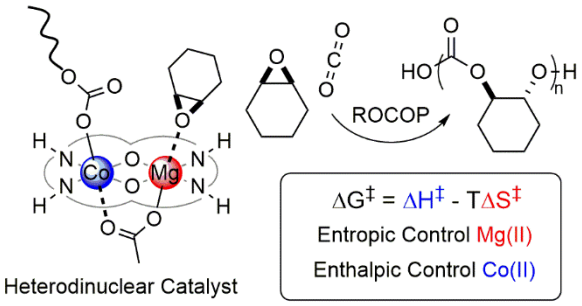

The copolymerization of CO_2 with epoxides is an attractive approach for valorizing waste products and improving sustainability in polymer manufacturing. Now, a heterodinuclear Mg(II)Co(II) complex has been show to act as a highly active and selective catalyst for this reaction at low CO_2 pressure. The synergy between the two metals was investigated using polymerization kinetics.